ELSEVIER

Materials Science and Engineering A325 (2002) 465–477

MATERIALS SCIENCE & ENGINEERING A

www.elsevier.com/locate/msea

Effects of ballistic impact damage on fatigue crack initiation in Ti–6Al–4V simulated engine blades

Christine M. Martinez [a], Daniel Eylon [b,*], Theodore Nicholas [c], Steven R. Thompson [c], John J. Ruschau [d], Janine Birkbeck [b,d], William J. Porter [d]

[a] *University of Dayton, Materials Engineering, Dayton, OH 45429, USA*
[b] *University of Dayton, Graduate Materials Engineering, 300 College Park, Dayton, OH 45429-0240, USA*
[c] *Air Force Research Laboratory, AFRL/ML, Wright–Patterson AFB, Dayton, OH 45433, USA*
[d] *University of Dayton Research Institute, Dayton, OH 45429, USA*

Received 7 August 2000; received in revised form 29 May 2001

Abstract

The ingestion of debris into jet engines creates nicks and dents on the leading edges of blades and vanes. This is commonly known as foreign object damage (FOD). Such damage, which can often result in premature failure, was simulated in the laboratory using diamond cross-section axial fatigue samples that were impacted with 1 mm diameter glass beads at 305 m s^{-1} at either 0 or 30° angle of incidence. The samples had either a thin leading edge (LE) with a radius of 0.127 mm or a thick LE with a radius of 0.381 mm. Fatigue strength of impacted specimens showed degradation of 10–50% due to LE damage, regardless of the depth of the damage zone. FOD related impact notch depth, loss of material (LOM), shear, folds, embedded shattered glass, and microstructural damage were characterized by SEM. Fatigue strength degradation was found to be higher for the 30° impacts than for the 0° impacts. No clear correlation between notch depth or LE thickness and fatigue strength was found.

Keywords: Ballistic impact; Fatigue strength; Damage characterization; Titanium; Foreign object damage

1. Introduction

A major cost and safety concern for military and commercial gas turbine engines is damage caused by the ingestion of foreign debris [1], commonly referred to as foreign object damage (FOD). Service experience has shown that FOD appears as nicked and dented blades or vanes, with depths of about 0.076 mm or less when it is the result of sand ingestion. FOD is known to reduce the service life of components exposed to vibratory loading [2], such as the engine blades shown in Fig. 1. As a result, FOD engine inspections based on defect depth measurement [3] have been implemented into engine maintenance plans. When leading edge damage depth exceeds the serviceability limit, it is blended out by filing [3].

Publications on research dealing with FOD on typical leading edge geometries or on real blades have been few and far between. Kaufman and Meyer [4] showed in the 1950s that smooth edge dents along the leading edge of actual compressor blades were less damaging, in terms of fatigue, than were sharp, irregular nicks of comparable size. This raised the question as to whether depth measurements alone offer much information on fatigue resistance of FOD damaged components. It was noted that the morphology or appearance of the FOD plays a larger role in establishing a fatigue debit. Nicholas et al. [5] studied the effects of FOD on titanium leading edges in the low cycle fatigue regime and found that, for each of four impact testing conditions, FOD related fatigue life debit followed the trend of data for a machined notch with a specific value of stress concentration factor, K_t. However, the morphology for the conditions evaluated in that work consisted of tears and loss of mass in addition to dents. It was

* Corresponding author. Tel.: +1-937-2292679; fax: +1-937-2293433.
E-mail address: eylon@udayton.edu (D. Eylon).

0921-5093/02/$ - see front matter
PII: S0921-5093(01)01532-5

found that dents or loss of material (LOM) through perforation were the least detrimental types of damage, while dents with tears were the most damaging. Some recent impact studies have been conducted on rectangular cross-section bars [6,7]. Peters et al. [6] studied the effects of FOD on the high cycle fatigue (HCF) threshold by shooting steel spheres onto the flat surface of rectangular specimens. They found that FOD can markedly reduce the fatigue life, compared with undamaged smooth-bar specimens, by providing sites for premature fatigue crack initiation. In another investigation, Hamrick [7] evaluated the effects of FOD on both diamond cross-section and uniform rectangular cross-section samples damaged by ballistic impact or by quasi-static indentation. He found that these two different impact methods created distinctly different damage mechanisms. It was suggested that a total damage depth parameter could be utilized to provide simple, reproducible and inexpensive methods for lab simulation of FOD, such as the quasi-static chisel indentations, to replace ballistic impact. However, in the present investigation, ballistic impact was chosen to simulate actual service conditions, and no attempt was made to use an equivalent quasi-static method.

In order to understand the effects of FOD on high cycle fatigue strength of engine blades, FOD was simulated in a laboratory environment on characteristic material and geometries representing the leading edge of engine blades using service-like sand ingestion impact conditions. The goal was to quantify the various damage parameters and determine their role in controlling the fatigue strength in Ti–6Al–AV simulated blades.

2. Materials and procedures

Samples were machined from Ti–6Al–4V forgings representative of gas turbine engine blades. The alloy was melted and rotary forged to a 6.35 cm diameter billet followed by mill annealing at 704 °C for 2 h and then air cooling in accordance with AMS 4928. The billet was next sectioned into forging multiples, 40.7 cm. in length which were preheated to 938 °C for up to

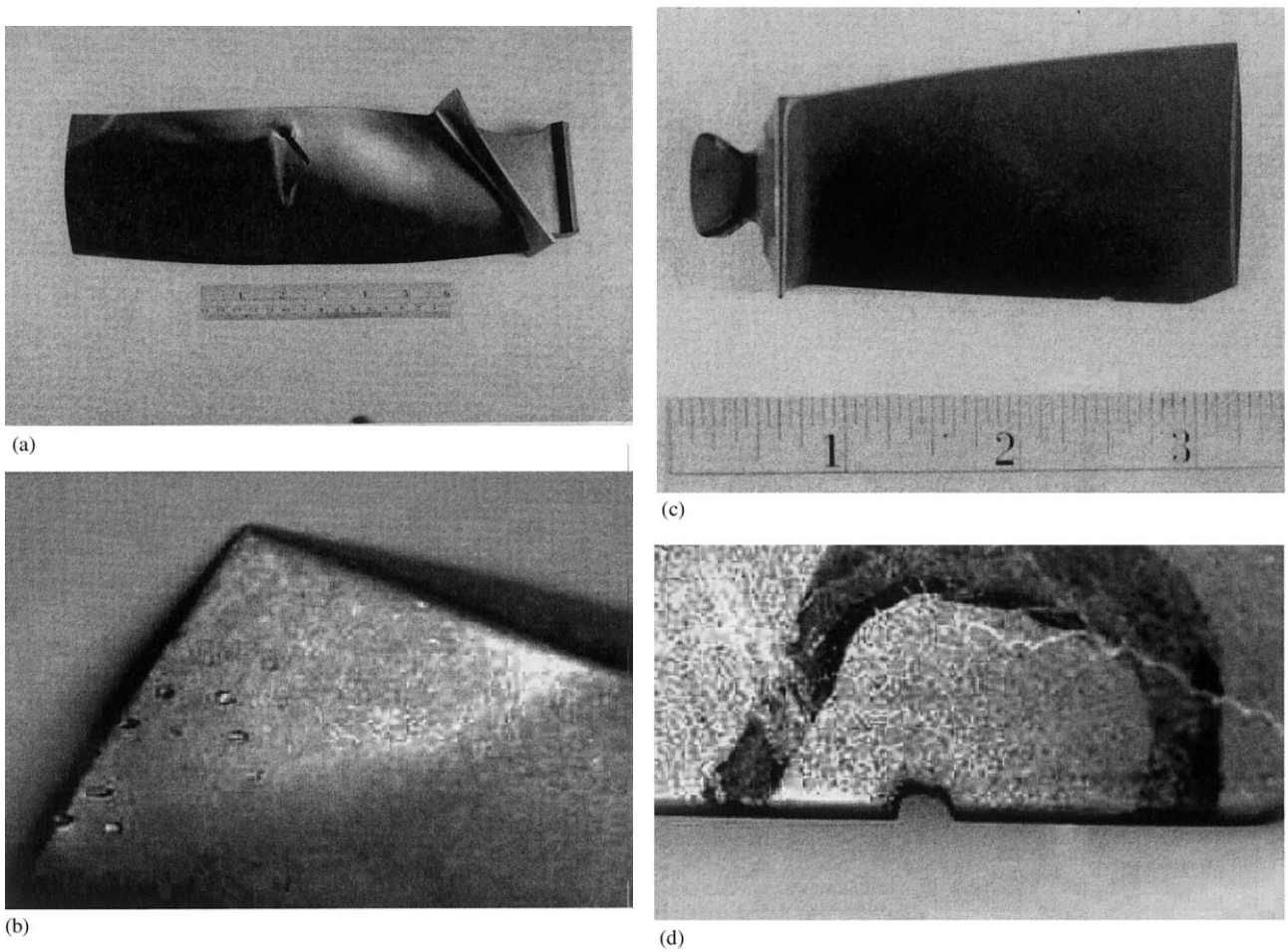

Fig. 1. Representative in-service FOD in a fan (a and b) and a compressor blade (c and d). (a) Fan rotor blade, (b) Close-up of (a), (c) Compressor rotor blade, (d) Close-up of (c).

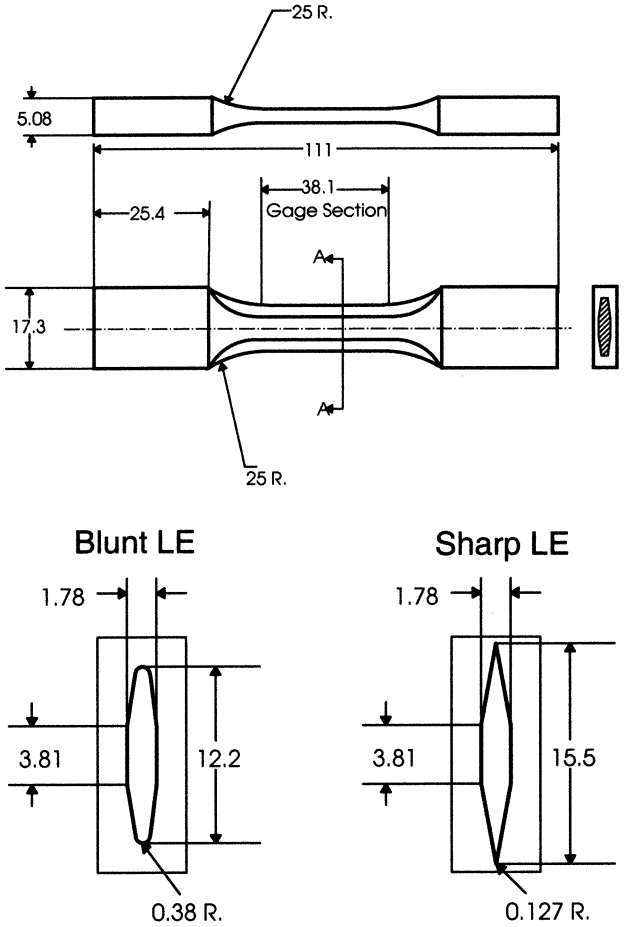

Fig. 2. Diamond cross-section test specimen, dimensions in millimeters (mm).

one hour prior to being pressed into their final channel-die forging dimensions of $40.7 \times 15.2 \times 2.0$ cm. The forgings were removed from the press and air-cooled. This processing resulted in a microstructure consisting of about 50 vol.% of equiaxed primary alpha with an average grain-size of 20 μm and a 50 vol.% of small colonies of lamellar alpha shown in earlier work [2,8]. Room temperature tensile properties of the final Ti–6Al–4V plate in the longitudinal direction displayed a yield stress, σ_y, of 930 MPa, and an ultimate tensile stress, σ_{UTS} of 978 MPa [2].

2.1. Specimen and ballistic impact

Two diamond cross-section specimen geometries, designed to simulate compressor airfoil leading edges, were machined to represent a 'thin' leading edge (LE) and a 'thick' LE geometry, shown in Fig. 2. The radius of the thin LE specimens was 0.127 mm and the thick LE radius was 0.381 mm [8].

A single-stage compressed-gas gun was used to ballistically impact the samples at the Impact Physics Laboratory of the University of Dayton Research Institute. Each specimen was impacted on each of the two leading edges with 1 mm diameter glass beads to simulate sand and grit impacts experienced in service. The glass beads were shot at 0 or 30° incident angles to simulate the typical range of fan and compressor blade FOD impact angles [9]. The beads were shot at 305 m s^{-1}, which approximates, the airflow speed of a foreign object relative to the blade during takeoff and landing, during which most FOD occurs [9]. Each of the samples' leading edges was impacted with one shot, thus producing two separate notches representing two potential crack initiation sites per sample. Both notches on a given sample, had the same angle of incidence but were deliberately offset on different planes so a crack would not necessarily go through both notches. The glass spheres typically shattered upon impact.

2.2. Fatigue testing

Fatigue testing was conducted on a custom-built test system utilizing an electrodynamic shaker for the dynamic load with a pneumatic chamber for applying the mean load. Stress ratios of $R = 0.1$ and 0.5 were chosen for this study to represent typical idle and peak loading conditions near the root of inservice blades [3]. Samples were subjected to tension-tension axial fatigue at 350 Hz. The test procedures and results of fatigue testing, correlating fatigue strength to impact conditions, have earlier been documented by Ruschau et al. [8]. Some of those results are summarized here for reference purposes.

2.3. Notch characterization

Prior to fatigue testing, most samples were characterized using a scanning electron microscope (SEM) for initial FOD impact damage. The damage features characterized included, *notch depth*, *material loss* on the notch surface, material *shear*, material *folding* over the LE, and *microstructural damage* such as deformed grains. The notches were photographed prior to testing, using a variety of orientations. These were (a) normal to the leading edge (Fig. 3a), (b) in the direction of impact (Fig. 3b), (c) profile of the leading edge (Fig. 3c), and (d) profile of the notch (Fig. 3d). The profile views in (c) and (d) are perpendicular to views (a) and (b), respectively. Fig. 4 shows the views taken at a fatigue-failed notch with a 30° impacted thin LE. The normal and profile views in (a) and (b) are taken before fatigue testing. The remaining views, (c) through (f) were taken after failure. Sections 'A' and 'B' identify the two halves of the broken sample. In addition to these views, the broken samples were tilted 30° along the length of the LE to view the notch/fracture interface as seen in Fig. 5. This view provided insight into the location and nature of the crack initiation, especially at higher magnifications.

3. Results and discussion

A total of 26 specimens, each with two notches of the same angle of incidence, were tested and characterized. They were grouped into four batches based on leading edge geometry and fatigue test stress ratio as summarized in Table 1. Each batch contained samples with both 0 and 30° shots.

All impacted samples exhibited a noticeable decrease in fatigue strength. This is as expected since the impacts produce a notch which results in a stress concentration factor larger than 1. The 0° impacts appear to have less fatigue strength degradation than the 30° impacts (Fig. 6). A surprising observation was the slightly higher fatigue strength of the thin LE samples than that obtained in the thick LE, samples, both subjected to similar FOD impacts. However, data scatter may imply that the thin LE samples were statistically no worse than the thick ones.

Preliminary finite element analysis, conducted by Weeks [10], indicated that 0° impact may leave behind residual compressive stresses in the notch root area. This could result in a relative improvement in crack initiation resistance at that location, when compared with 30° impacts. The latter may have developed a gradient of residual stresses across the notch area in the direction of impact [10], ranging from compression at the exit side bulge to tension at the rim of the entrance side. The 30° impacts show a distinct projectile entrance and exit location in the notch area (Fig. 3b) that might have produced such a residual stress gradient.

Approximately, 80% of the 0° shots fired at the thin LE samples hit the leading edge slightly off center and were deflected. Photographs of representative 0° impacts for both the thin and the thick edges can be found in [11]. The deflected shots created little damage to the leading edge while producing a dent similar to what is observed in the 30° shots. While the material was shifted to one side, the magnitude of the residual compressive and tensile stresses is not necessarily identical to that of the 30° shots, as discussed above. This may be one reason why the 0° impact samples showed slightly higher fatigue strength than the 30° impact samples (Fig. 6), especially for the thin edge samples. In

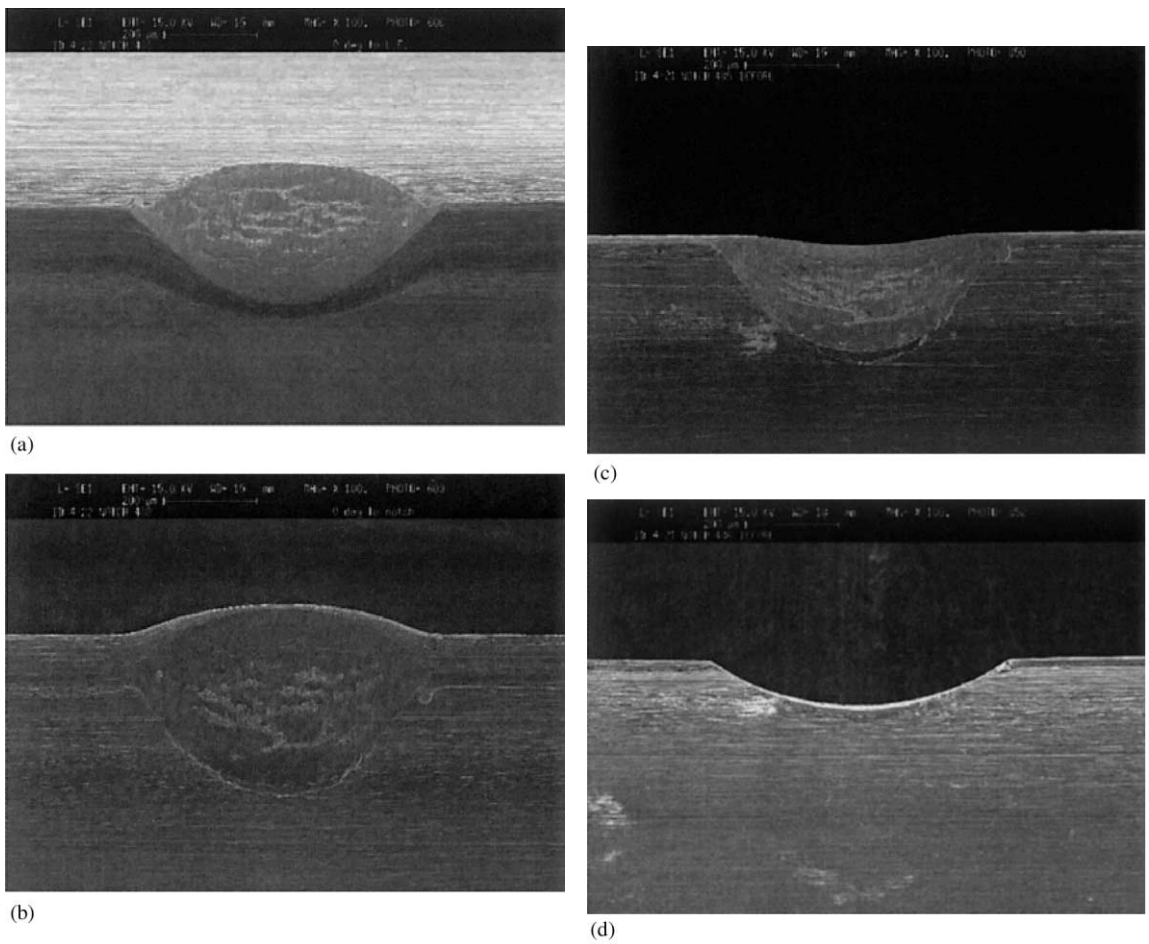

Fig. 3. (a) Un-failed notch for sample 4-22, with a thin LE and a 30° impact. Normal to LE. (b) Un-failed notch for sample 4-22, with a thin LE and a 30° impact. In the direction of impact. (c) Un-failed notch for sample 4-22, with a thin LE and a 30° impact. Profile of LE. (d) Un-failed notch for sample 4-22, with a thin LE and a 30° impact. Profile of notch.

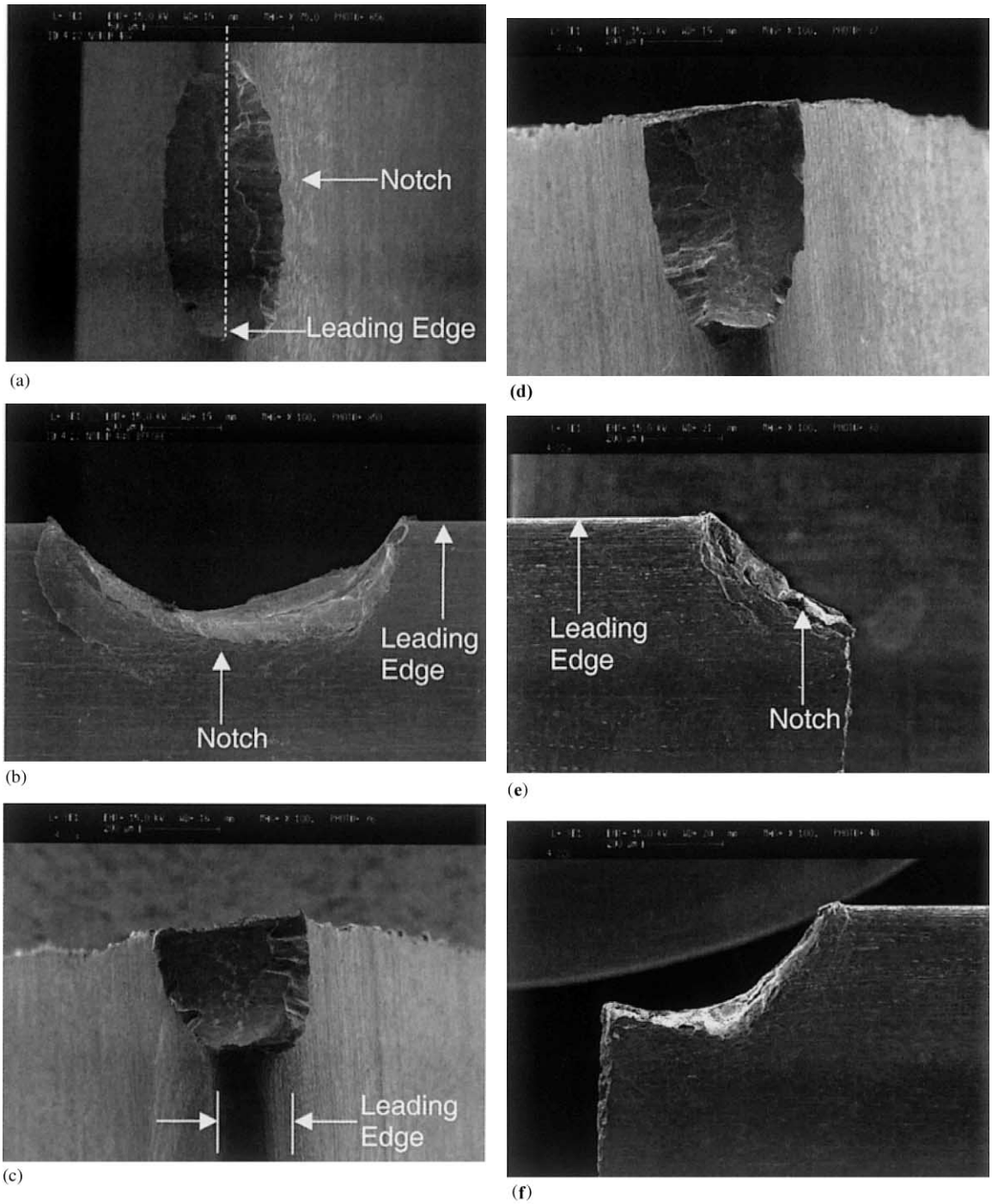

Fig. 4. (a) Failed notch for sample 4-22. Normal to LE and notch. (b) Failed notch for sample 4-22. Profile to LE and notch. (c) Failed notch for sample 4-22. Normal to LE and notch, Section A. (d) Failed notch for sample 4-22. Normal to LE and notch, Section B. (e) Failed notch for sample 4-22. Profile to LE and notch, Section A. (f) Failed notch for sample 4-22. Profile to LE and notch; Section B.

this case, there might be a higher level of residual compressive stresses and lower residual tensile stresses than in a typical angled impact, because the bead compresses the material to one side instead of shearing it from entrance to exit. Another consideration is the competing effects of a stress concentration at the depth of the notch versus the effects of a tensile residual stress at a different location, each of which would tend to be the location of a fatigue failure.

Since the thick LE presented a wider target, 25% of the 0° impacts hit it head-on, while the remaining 75% resembled the 30° impacts on edges, shown in Fig. 7. The stiffness of the thick LE prevents it from deflecting to the side as much as the thin LE for either impact angle. Due to the head-on nature of the impact, these might have produced less residual stress due to the

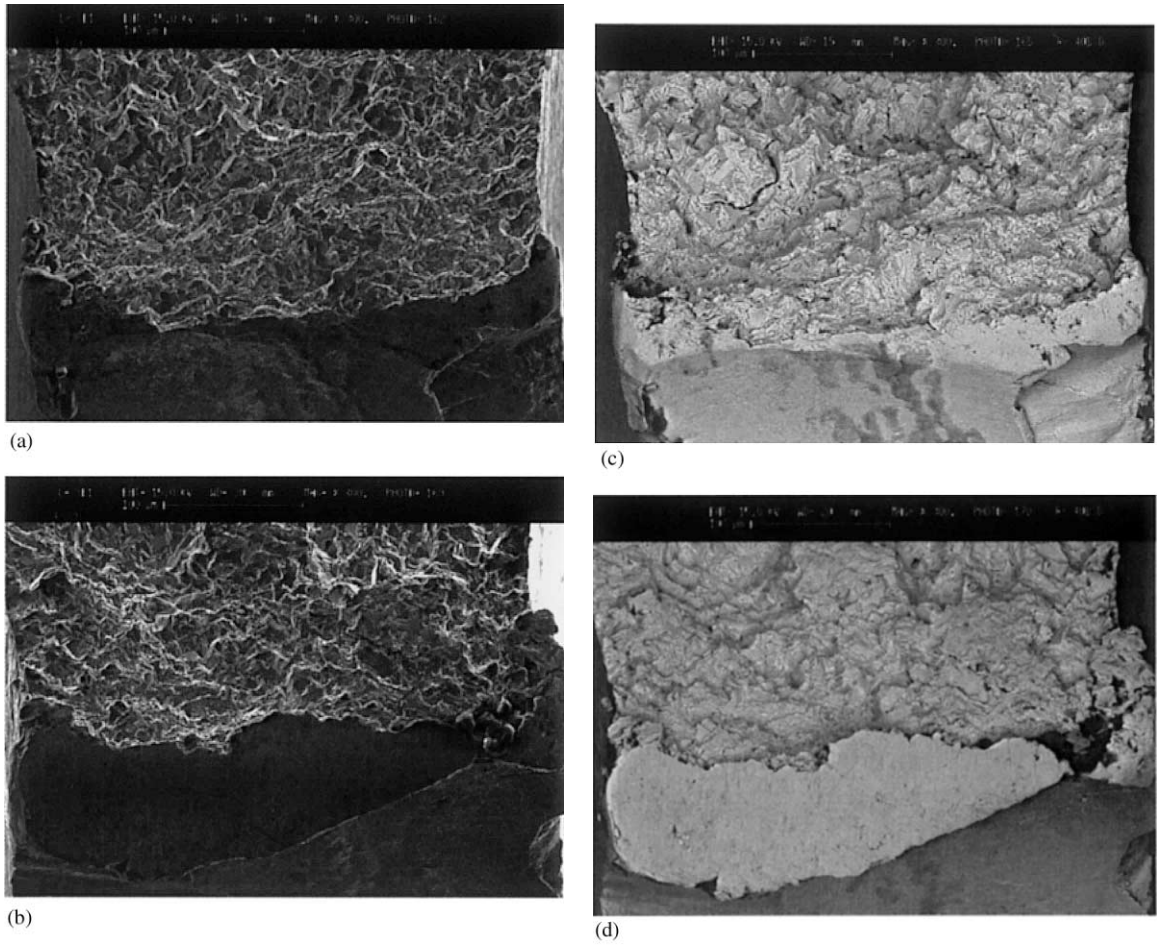

Fig. 5. (a) Fracture views of failed notch for sample 4-22. Fracture/notch view; Section A. (b) Fracture views of failed notch for sample 4-22. Fracture/notch view; Section B. (c) Fracture views of failed notch for sample 4-22. Fracture/notch view; Section A. backscatter detector photograph. (d) Fracture views of failed notch for sample 4-22. Fracture/notch view; Section B. backscatter detector photograph.

larger mass resisting the impact. Thus, the results show a greater reduction in strength on the thick edge than on the thin edge. The similarity in fatigue strength debit between the 0 and 30° impacts for the thick LE could be due to the fact that the damage from 0° impacts resembles that of damage from 30° impacts because of the minimal sidewise deflection.

3.1. Characterization of damage features

The features, resulting from the ballistic impact, that were characterized include the *notch depth*, *LOM* on the notch surface, *microstructural damage* such as deformed grains, and other damage features such as *material shear*, *material folding* over the LE, and *embedded glass* from the shattered bead.

3.1.1. Effects of notch depth

The notch depth was measured by rotating the SEM stage to achieve a profile view of the notch, as shown in Fig. 8. These two notches are from the same sample and were impacted at 30°. Fig. 8a is an example of a shallow notch with no LOM (dent), while Fig. 8b shows a deeper notch with loss of material.

Fig. 9 plots a comparison of the depth of the failed notch, where crack initiation occurred, and the un-failed notch, for each specimen impacted at 0°. In a majority (65%) of the cases, when failure could be associated with a notch, initiation occurred at the deeper of the two notches. The average damage depth of failed notches is 0.20 mm while for un-failed notches it is 0.12 mm. Whereas the 0° impacts failed at the deeper notch 65% of the time, the 30° impacts failed at the deeper of the two 85% of the time, as shown in Fig.

Table 1
Samples characterized and the list of each condition

Batch	LE	Stress ratio	Number of 0° samples	Number of 30° samples
1	Thin	0.1	2	6
2	Thin	0.5	2	3
3	Thick	0.1	2	4
4	Thick	0.5	2	5

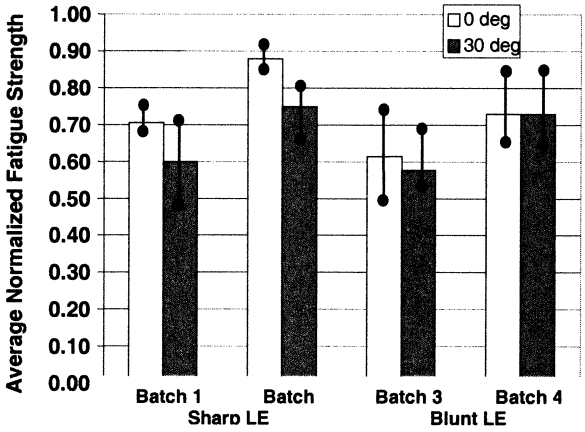

Fig. 6. Average normalized fatigue strength of batches 1 through 4.

10. For these tests, Ruschau et al. [8] showed that in spite of the preferred initiation at the deeper of the two notches for a given sample, the depth of the failed notch had no significant effect or systematic trend with respect to the normalized fatigue strength. These results challenge some of the engine inspection and maintenance practices currently used by various aviation authorities.

3.1.2. Effects of loss of material (LOM)

Another feature observed was the LOM from the surface of the notch, which was found on 65% of the failed notches and only 20% of the un-failed notches. Fig. 11a illustrates a shallow notch with no material loss and a smooth surface (see also Fig. 8a). This is a 30° impact, where the bead seems to have only 'dented' the leading edge. On the other hand, Fig. 11b shows a rough and jagged notch where there is material loss (see also Fig. 8b). Crack initiation always occurred at the deeper notch exhibiting LOM.

In Fig. 12, an attempt was made to correlate the LOM of the failed notches to the average normalized fatigue strength. LOM for 30° impacts shows highly scattered results indicating that LOM alone has no clear effect on fatigue strength. Note that the determination of LOM is highly subjective and not very quantitative. However, there is a general trend for the 0° impacts showing lower average normalized fatigue strength with higher LOM. Unfortunately, only two

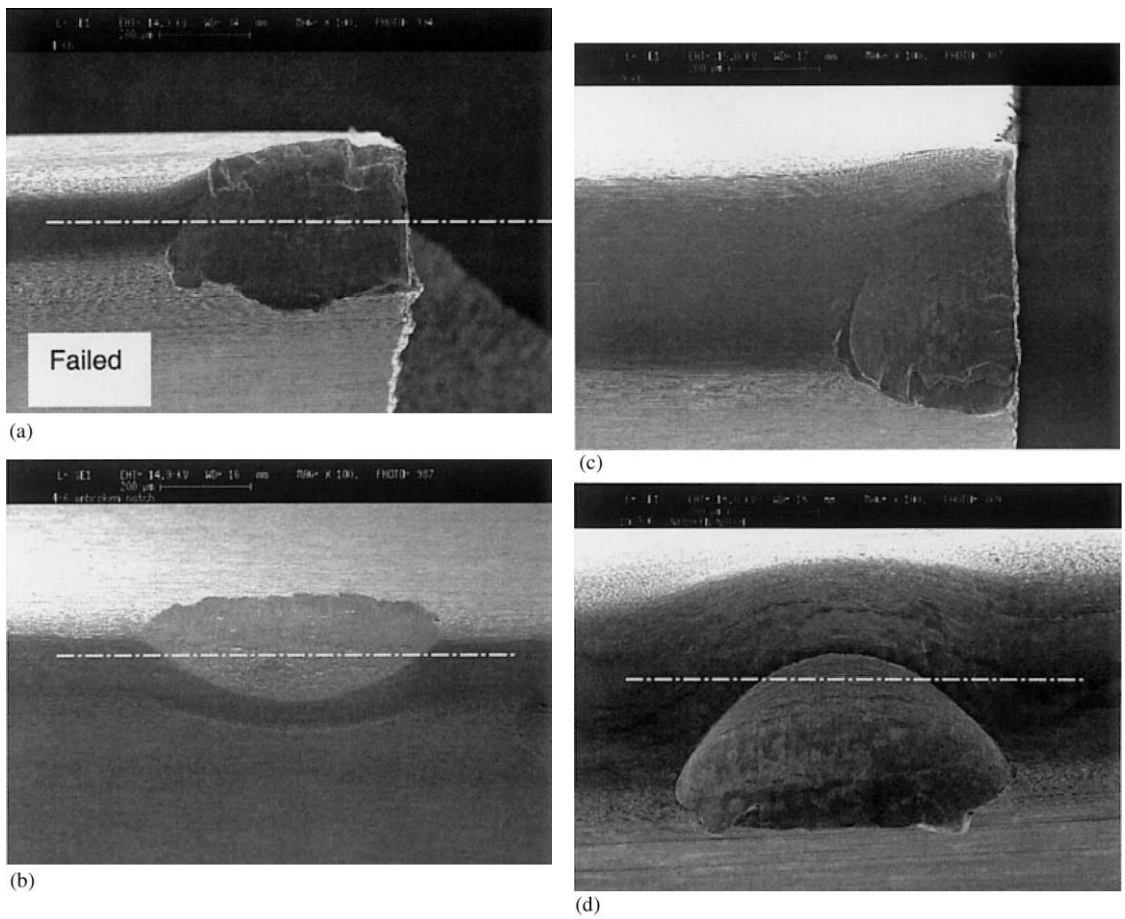

Fig. 7. (a) Samples with 30° impacts. ID 4-6 sample with thin LE, failed notch. (b) Samples with 30° impacts. ID 4-6 sample with thin LE, un-failed notch. (c) Samples with 30° impacts. ID 9-6 sample with thick LE, failed notch. (d) Samples with 30° impacts. ID 9-6 sample with thick LE, un-failed notch.

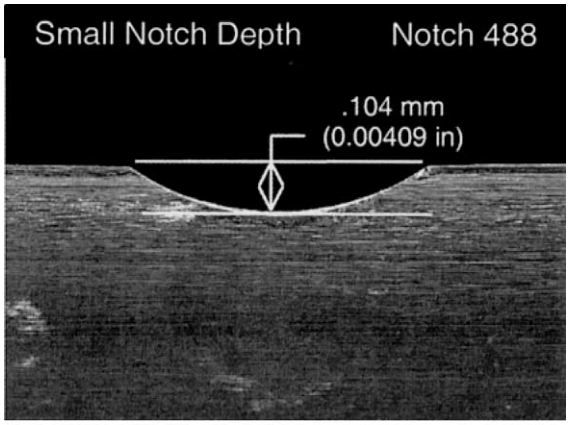

(a)

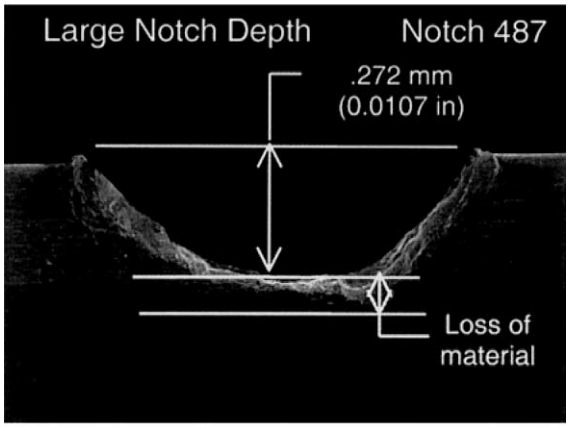

(b)

Fig. 8. (a) Characteristic notch depth (thin LE with a 30° impact, sample 4-22). Shallow notch with no material loss. (b) Characteristic notch depth (thin LE a 30° impact, sample 4-22); a deep notch with material loss.

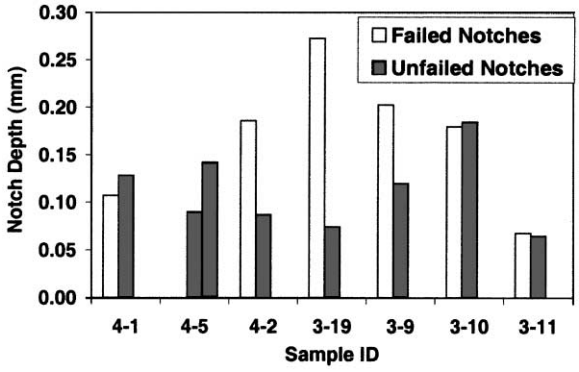

Fig. 9. Depth of failed vs. un-failed notches for 0° impacts in both thin and thick LE. (In sample 4-5, failure occurred outside of the notches).

out of eight 0° impacts actually hit head-on to the LE (Fig. 12b c). The remaining six impacts slightly missed the edge and created an abnormal impact, seen in Fig. 12a. However, these observations are slightly obscured because the HCF strengths are so highly scattered. Even though the amount of LOM may not have a direct effect on the loss of fatigue strength, the result of such damage can produce sharp edges and micro-folds on the surface of the notch. In addition, it is possible that the material removal also relieved the residual compressive stresses in that area. Most samples failed at

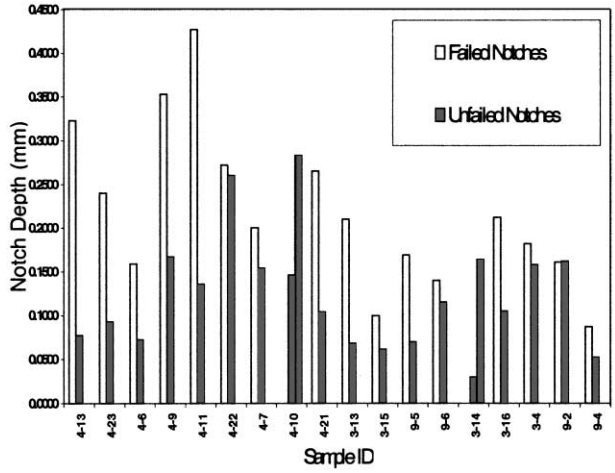

Fig. 10. Depth of failed vs. un-failed notches for 30° impacts for both thin and thick LE.

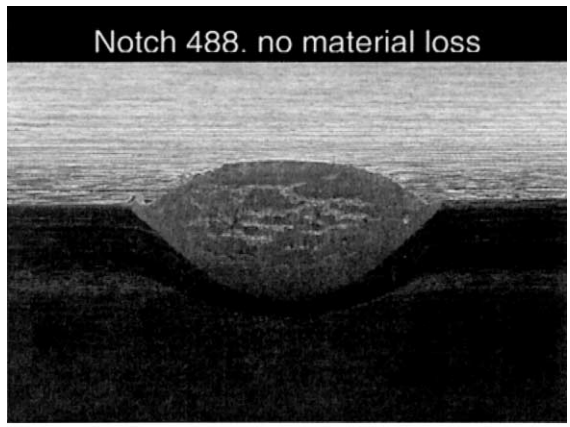

(a)

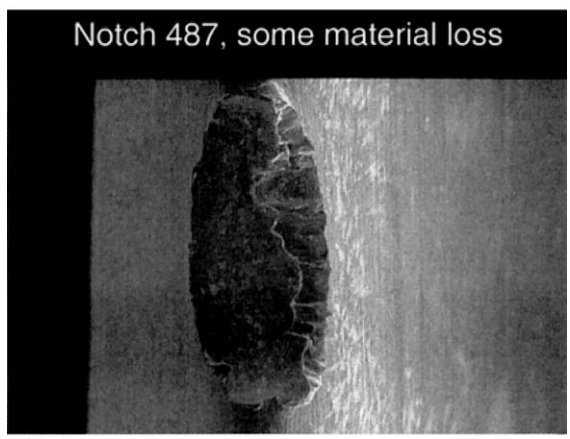

(b)

Fig. 11. (a) Loss of Material (thin LE with a 30° impact, sample 4-22). (b) Loss of Material (thin LE with a 30° impact, sample 4-22).

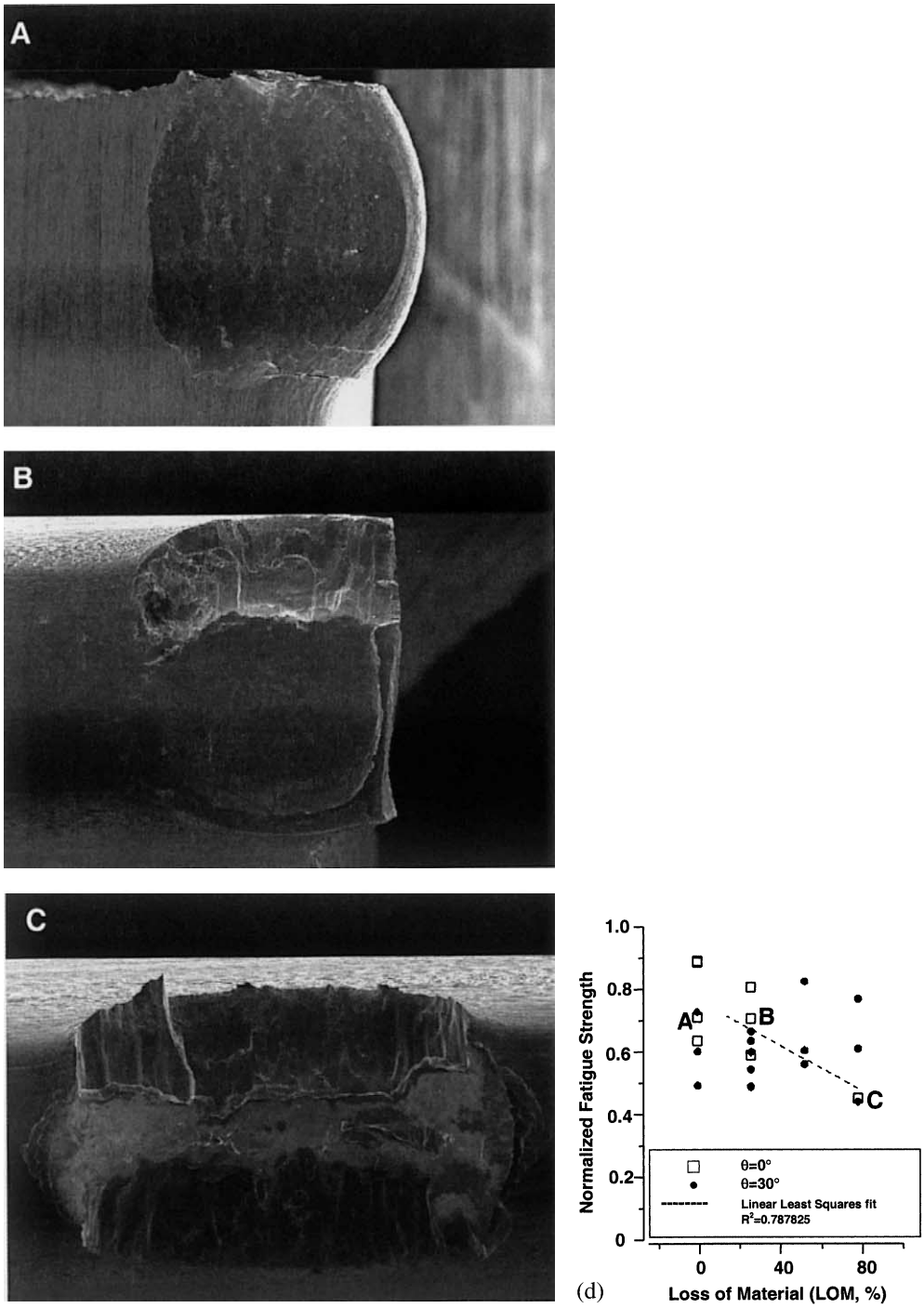

Fig. 12. Comparison of materials loss and the fatigue strength; linear least squares fit for 0° impacts for both thin and thick LE. (a) Thin LE correlates with data point A. (b) Thin LE correlates with data point B. (c) Thin LE correlates with data point C.

the notch with LOM, 81% of the 30° impacted samples failed at the notch with LOM, and 75% for the 0° impacted samples.

In most cases LOM provides a suitable crack initiation site for failure to occur. Fig. 13 illustrates the fracture surface for sample 3–19 (shown also in Fig. 12c), with a large amount of LOM. In addition to the LOM, the notch contained embedded glass from the shattered bead. The crack did not initiate at the embedded glass, but at a slight fold in the LOM section of the notch denoted by the circle. The depth of this notch was 0.273 mm (0.0107″) and the fatigue strength debit of this sample was 49% of an un-notched sample.

3.1.3. Effects of microstructural damage

Precision micro-sectioning was performed on selected samples as shown in Fig. 14. These photomicrographs

were taken at the mid-plane of a fractured sample with a 53% fatigue strength debit and a notch depth of 0.21 mm. Evident from each photo is a band of deformed grains along the periphery of the notch, typically 60–100 μm wide. While there was no evidence of subsurface cracking in the direction of eventual crack growth in any of the samples examined, multiple shear bands roughly parallel to the notch were observed in all of the micro-sectioned samples. The orientation of these bands, parallel to the applied loading direction (perpendicular to eventual fatigue cracking and to the impact direction), indicates that their presence may have had little influence on the fatigue life.

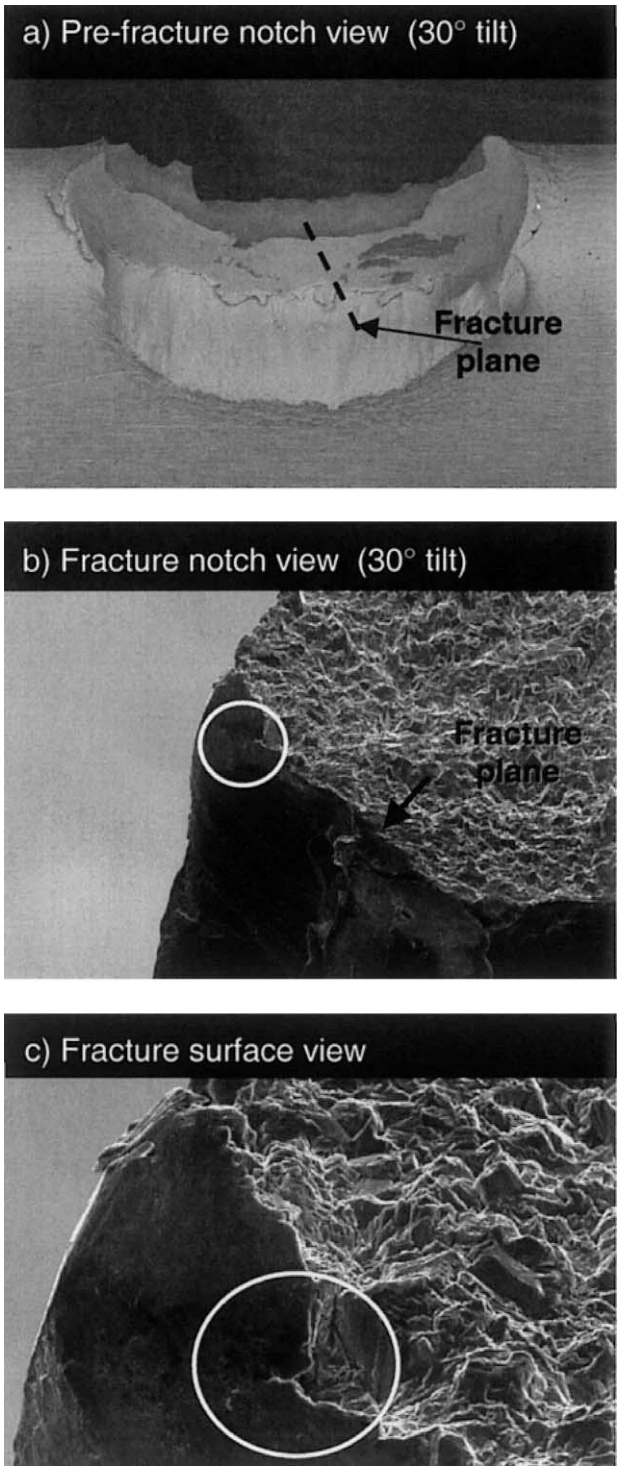

Fig. 13. (a) Fracture initiation of sample 3-19 (thick LE with a 0° impact). (b) Fracture initiation of sample 3-19 (thick LE with a 0° impact) (c) fracture initiation of sample 3-19 (thick LE with a 0° impact).

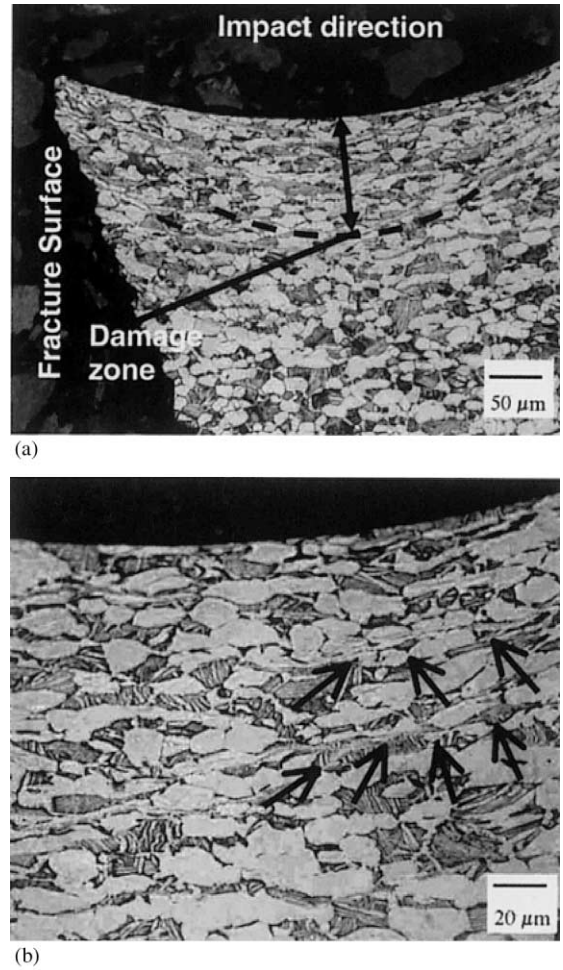

Fig. 14. Precision micro-sectioning of sample 3-13, thick LE, 30°impact; (b) Precision micro-sectioning of sample 3-13, thick LE, 30° impact.

3.1.4. Effects of other impact features

Other damage features included *material shear* in the notch region (Fig. 15a and b), *material folding* over the LE (Fig. 15c), and *embedded glass*, confirmed by energy dispersive spectroscopy, from the shattered bead (Fig. 15d). None of these features alone appeared to have any significant effect on the loss of fatigue strength. On the other hand, the combination of shearing and folding provided suitable crack initiation sites for some of the samples. Fig. 16 illustrates the fracture of sample 3–4, which had a notch depth of 0.182 mm (0.007″) and a fatigue strength loss of 64%. The pre-fracture

condition of the notch indicates a material shear (or tearing) marked by the circle in Fig. 16a. The post-fracture condition of the notch shows that the fracture initiated somewhere behind the material shear, Fig. 16b and c.

3.2. Initiation location in the impact notch

Early research shows that fatigue failures of samples ballistically damaged with larger steel balls at similar velocities initiated at the edge (rim) of the notch [6,7]. In the present investigation, it was found that fatigue cracks generally initiated in the central region of the notch (indicated by the 0.25–0.50–0.25 region in Fig. 17). Regardless of the notch condition (notch depth, LOM, shearing, or embedded glass), failure occurred at or near the center of the notch for 30° impacts. There is no clear correlation for 0° impacts, partially due to data scatter and the limited number of data points, as seen in Fig. 18. The difference in the failure sites between this and earlier work may be the heavier steel ball used and the resulting impact damage in the earlier studies. In addition, Ti–6Al–AV flat specimens were used in the earlier research and were impacted on the flat surface of a larger fatigue specimen as opposed to this investigation in which thin samples were impacted on the edge; the latter being more representative of an actual airfoil edge.

4. Summary and conclusions

High-cycle fatigue testing of Ti–6Al–4V simulated airfoil samples, each with two ballistic impact notches, showed fatigue strength degradation as a result of impact edge damage. Impact damage was quantified by measuring the notch depth, LOM at the notch, material shear, material folding over the LE, embedded glass fragments, and microstructural damage. A combination of notch stress concentration and impact residual stresses appear to play a dominant role in fatigue strength degradation. However, insufficient data in this

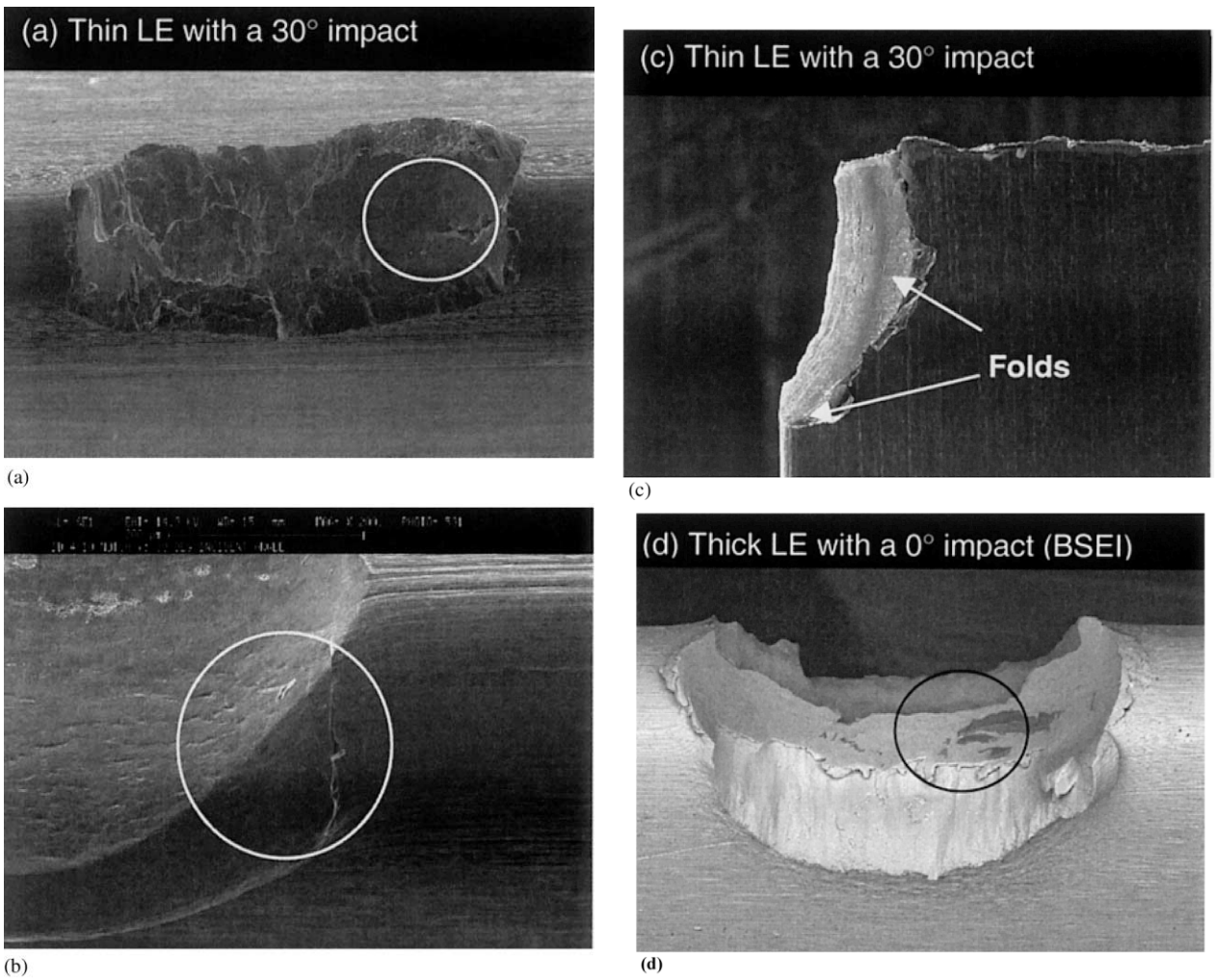

Fig. 15. (a) Material shear. (b) Another form of material shear. (c) Material fold. (d) Embedded glass.

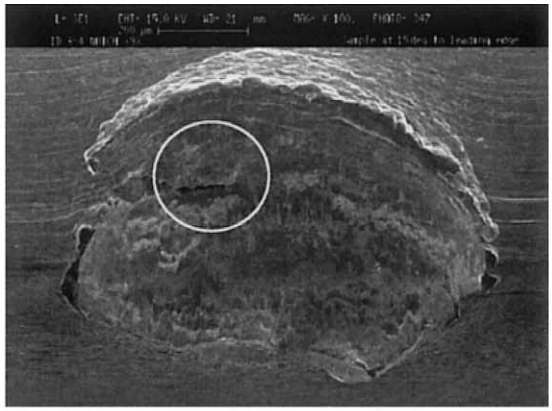

(a)

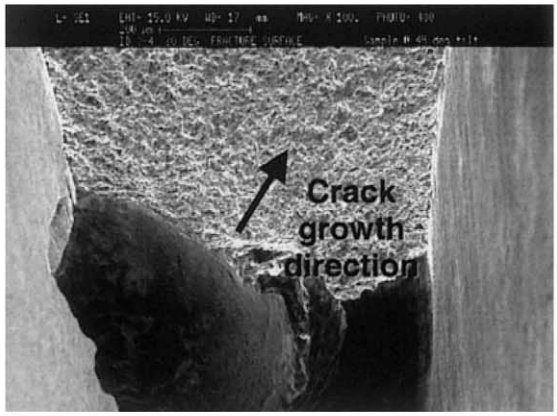

(b)

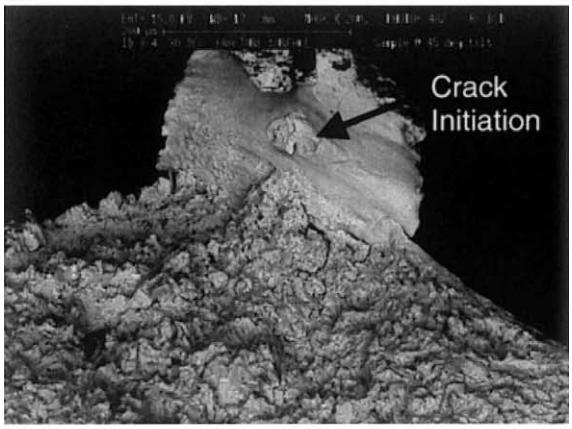

(c)

Fig. 16. Before fracture picture of sample 3-4 with a thick Le and a 30° impact, material shear parallel to LE. (b) After fracture photo. (c) After fracture photo behind material shear.

study preclude the making of a definitive statement. Generally, samples with a 30° angle of incidence had a higher fatigue strength debit than those with 0° impacts. This is attributed to the development of a complex residual stress field that includes tension on the incoming side of the impacting projectile. Fracture initiation generally occurred at the deepest of the pair of notches for most of the samples, both at 0 and 30° incident angles. In addition, initiation generally occurred at the deepest section of the notch. Surprisingly, the depth of the failed notch had no apparent direct effect on the fatigue strength. LOM for 30° impacts showed highly scattered results indicating that LOM alone has no direct effect on the fatigue strength. The data for the 0° impacts, on the other hand, showed a general trend of lower fatigue strength for higher LOM. Of the 30° impacted samples, 81% failed at the notch with LOM, as did 75% of the 0° impacted samples. Even though LOM itself cannot be directly correlated to fatigue strength debit, the result of such damage produced sharp edges and micro-folds on the surface of the notch, which could have provided sites for crack initiation. The same is true for material shear and folds, but not for embedded glass. Regardless of the notch condition (depth, LOM, shearing, or embedded glass), failure occurred at or near the center of the notch for 30° impacts, but there was no clear correlation for 0° impacts, partially due to data scatter and a limited number of data points.

Precision micro-sectioning showed microstructural shear bands which are oriented parallel to the applied loading direction (perpendicular to eventual fatigue cracking and the impact direction). The role of these shear bands on fatigue strength is believed to be benign

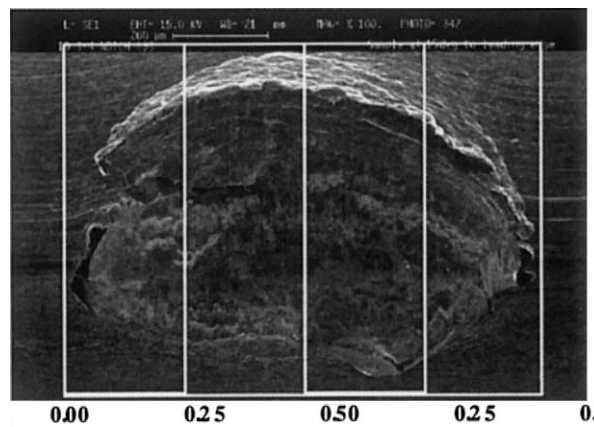

Fig. 17. Photograph showing location of crack initiation.

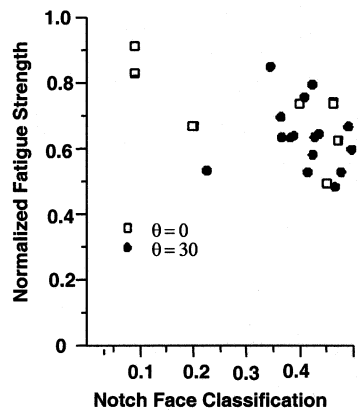

Fig. 18. Influence of crack initiation location on fatigue strength.

because of their orientation with respect to the fatigue loading direction.

Acknowledgements

The authors wish to acknowledge the support of Eric Fletcher, Bob Lewis, and Luann Piazza of Universal Energy Systems, Dayton, OH, for their substantial contributions to this research. The lead author would like to recognize the members of the 20th Fighter Wing at Shaw AFB who provided a world of insight into FOD inspection in the field; with special thanks to MSgt. Michael Sartain, TSgt. David L. Harrington, TSgt. Covington, and SSgt. Canning. Thanks are also due to the Dayton Area Graduate Studies Institute (DAGSI) for their financial support of C.M. Martinez and J. Birkbeck at the University of Dayton and to the National Turbine Engine High Cycle Fatigue program for providing the research support for this study. The work described herein was conducted at the Air Force Research Laboratory, Materials and Manufacturing Directorate, Wright–Patterson AFB, OH, USA.

References

[1] T. Nicholas, Int. J. Fatigue 21 (1999) 221–231.
[2] D.B. Lanning, G.K. Haritos, T. Nicholas, Int. J. Fatigue 21 (1999) 643–652.
[3] Technical orders 1F–16CJ–2–70FI–00–1 for the F11O–GE–129 engine. 10-41–10-84.
[4] A. Kaufman, A.J. Meyer Jr, National Advisory Committee for Aeronautics, Technical Note 3275, June 1956.
[5] T. Nicholas, J.P. Barber, R.S. Bertke, Exp. Mech. 20 (1980) 357–364.
[6] J.O. Peters, O. Roder, B.L. Boyce, A.W. Thompson, R.O. Ritchie, Metall.Metals Trans. 31A (2000) 1571–1583.
[7] Joseph L. Hamrick, Major, USAF, Ph.D. Dissertation, Air Force Institute of Technology, September, 1999.
[8] J.J. Ruschau, T. Nicholas, S.R. Thompson, Int. J. Impact Eng. 25 (2001) 233.
[9] Dr. Richard Bellows, Allied Signal Engine Co., October 7, 1997, personal communication.
[10] C. Weeks, Allison Advanced Development Company, Indianapolis, Indiana, 1999, unpublished research.
[11] C.M. Martinez, M.S. Thesis, School of Engineering, University of Dayton, Dayton, OH, April, 2000. Also in Technical Report AFRL-ML-WP-TR-2000-4097, Wright–Patterson AFB, OH, April 2000.